HHS Public Access

Author manuscript

Nat Cell Biol. Author manuscript; available in PMC 2009 August 01.

Published in final edited form as:

Nat Cell Biol. 2009 February ; 11(2): 183–189. doi:10.1038/ncb1825.

UNC-6 (Netrin) Orients the Invasive Membrane of the Anchor Cell in *C. elegans*

Joshua W. Ziel[1], **Elliott J. Hagedorn**[1], **Anjon Audhya**[2], and **David R. Sherwood**[1,3,*]

[1]Department of Biology, Duke University, Box 90338, Durham, NC 27708 USA

[2]Department of Biomolecular Chemistry, University of Wisconsin-Madison, 1300 University Avenue, Madison, WI 53706

[3]Molecular Cancer Biology Program, Duke University Medical Center, Durham, NC 27708 USA

Abstract

Despite profound importance in development and cancer, the extracellular cues that target cell invasions through basement membrane barriers remain poorly understood 1. A central obstacle has been the difficulty of studying the interactions between invading cells and basement membranes *in vivo* 2,3. Using the genetically and visually tractable model of *C. elegans* anchor cell (AC) invasion, we show that *unc-6* (netrin) signaling, a pathway not previously implicated in controlling cell invasion *in vivo*, is a key regulator of this process. Site of action studies reveal that prior to invasion localized UNC-6 secretion directs its receptor, UNC-40, to the AC's plasma membrane in contact with the basement membrane. There, UNC-40 polarizes a specialized invasive membrane domain through the enrichment of actin regulators, F-actin and phosphatidylinositol 4,5-bisphosphate. Cell ablation experiments indicate that UNC-6 promotes the formation of invasive protrusions from the AC that break down the basement membrane in response to a subsequent vulval cue. Together, these results characterize an invasive membrane domain *in vivo*, and reveal a novel role for netrin in polarizing this domain towards its basement membrane target.

From its position within the developing uterus, the *C. elegans* anchor cell (AC) breaks through the juxtaposed gonadal and ventral epidermal basement membranes and inserts between the central 1° fated vulval precursor cells (VPCs) to mediate uterine-vulval connection (Fig. 1a, f) 4,5. AC invasion is regulated by *fos-1a*, the *C. elegans* ortholog of the Fos bZIP transcription factor. FOS-1A controls the expression of genes in the AC that mediate basement membrane breakdown6–8. Although required for invasion, FOS-1A is not sufficient to promote basement membrane removal. Breaching the basement membrane also depends upon a signal from the 1° VPCs that activates a FOS-1A-independent pathway that stimulates the extension of invasive processes from the AC's basal membrane 5. Neither the molecular identity of the vulval cue nor the mechanisms that control the polarized invasive response, however, are known.

---

*To whom correspondence should be addressed. E-mail: david.sherwood@duke.edu.

To identify signaling pathways that promote invasive protrusions, we examined *C. elegans* strains with mutations in genes important for cellular motility (Supplementary Information, Table S1) and found that animals harboring mutations in the guidance factor *unc-6* (netrin) or its receptor *unc-40* (DCC) showed the greatest defects in AC invasion. The netrin signaling pathway regulates numerous developmental events involving migrations through basement membrane 9, however, a direct role for netrin in regulating cell-invasive behavior has not been demonstrated. Examination of animals at the mid-to-late L3 stage (P6.p 4-cell) revealed that the AC failed to invade in *unc-6(ev400)* and *unc-40(e271)* mutants (Fig. 1b, see Table S2), and only approximately half completed a delayed invasion by the L4 stage (P6.p 8-cell; Table S2). Consistent with this receptor-ligand pair functioning together, *unc-40*; *unc-6* double mutant animals exhibited a similar invasion defect (Table S2). Inspection of *unc-6* and *unc-40* mutants prior to invasion indicated that in most cases the AC was situated normally over the vulval cells (n = 104/119 and 154/175 animals, respectively), demonstrating a specific invasion defect rather than an indirect consequence of AC mispositioning 10.

To determine whether *unc-6* might regulate the generation of invasive protrusions, we ablated all VPCs except the posterior-most P8.p cell in wild-type and *unc-6* animals. The descendants of these isolated P8.p cells adopt the 1° VPC fate (Fig. 1c, f), generate the stimulatory invasion cue, and then move towards the AC, providing an assay for the ability of the AC to extend invasive processes 5. In contrast to wild-type animals, which directed invasive processes from all distances examined (Fig. 1c), ACs in *unc-6* mutants never extended invasive protrusions, even when bordered by 1° VPCs (Fig. 1d, e). These experiments suggest that *unc-6* is either a component of the 1° vulval signal or is required for the formation of invasive protrusions in response to this cue.

Previous work has indicated that UNC-6 is expressed in neurons of the ventral nerve cord (VNC) from the L1 stage through the adult stage, but not in the 1° VPCs until the late L3 stage, after the AC breaches the basement membrane 11,12. We confirmed these studies using an *unc-6* transcriptional reporter (Fig. S1) and a rescuing Venus::UNC-6 transgene. Notably, in addition to previously reported expression, low levels of full length Venus::UNC-6 were observed in the basement membrane under the AC (Fig. 2a, b), likely originating from the VNC. Site of action studies revealed that VNC-specific expression of Venus::UNC-6 11 restored normal AC invasion in 90% of *unc-6* animals (Table S2). In contrast, Venus::UNC-6 driven expression in the 1° VPCs 13 (mirroring the predicted expression of the vulval cue) did not rescue invasion (Table S2), suggesting that the timing of expression or processing of UNC-6 by the 1° VPCs is not sufficient to stimulate invasion. Finally, 1° VPC-specific RNAi-mediated knockdown of *unc-6* (*egl-17>mrfp::rde-1*; *rde-1(ne219)*) did not cause AC invasion defects (Table S2) 11. These results suggest that UNC-6 is not the vulval cue, but rather a VNC-derived signal that promotes AC invasion.

To establish genetically whether *unc-6* functions as a separate non-vulval cue, we created vulvaless animals (see Methods) carrying the *unc-6* mutation. We have previously shown that approximately 20% of ACs invade in vulvaless animals (created by laser ablation or loss of vulval induction; Table S2; Fig. 2c) 5. If *unc-6* encoded the vulval cue or regulated its secretion, loss of *unc-6* would not enhance the invasion defect in vulvaless animals.

Alternatively, if *unc-6* was a distinct signal, its loss should augment the invasion defect of vulvaless animals. Supporting this second scenario, ACs in vulvaless animals harboring the *unc-6* mutation had a dramatically more severe invasion defect: ACs never invaded and most detached from the basement membrane (Fig. 2d; Table S2). Furthermore, removal of the vulval cells had no effect on UNC-6 expression or localization (Fig. S2). We conclude that UNC-6 is a separate VNC-derived signal that regulates AC invasion.

Expression of the UNC-6 receptor, UNC-40: :GFP, driven by an AC-specific cis-regulatory element (Fig. S3) 8 restored normal invasion in 96% of *unc-40* mutant animals (Table S2), demonstrating that UNC-6 signals directly to the AC to promote invasion. Beginning 5–6 hours before invasion, UNC-40: :GFP was found within intracellular vesicles and polarized along the AC's invasive plasma membrane (Fig. 3a–c). UNC-40: :GFP localization was normal in vulvaless animals (Fig. 3f), however, loss of *unc-6* resulted in the mislocalization of UNC-40: :GFP along lateral and apical membranes (Fig. 3d, f; Table S3). To determine whether the ventral presentation of UNC-6 is required to target AC invasion and UNC-40: :GFP localization, we drove ubiquitous expression of a hemagglutinin (HA)-tagged UNC 6 protein (UNC-6: :HA) under the control of the heat-shock promoter *hsp-16-2* prior to invasion (*hs>unc-6: :HA*) 14. Non-localized expression of UNC-6: :HA led to disruptions in AC invasion at all time points examined. The perturbations peaked four hours after heat-shock (Table S2), and resulted in mislocalized UNC-40: :GFP (Fig. 3e, f; Table S3). Thus, localization of UNC-40 to the invasive cell membrane is a specific targeting event mediated by UNC-6, and is required to promote invasion.

In neurons, signaling downstream of UNC-40 is mediated in part by the actin regulators UNC-34 (Ena/VASP) and the Rac GTPase, CED-10 15. Importantly, *unc-34* mutants had perturbations in AC invasion, as did animals carrying mutations in both *ced-10* and *mig-2*, a Rac homolog that often functions redundantly with *ced-10* 16 (Table S2), indicating a similar downstream network acts within the AC. To probe the relationships between these genes, the actin cytoskeleton and *unc-6*, we examined functional translational fusions of GFP to MIG-2 and CED-10, as well as AC-specific expression of GFP tagged UNC-34 and the filamentous Actin Binding Domain of the *moesin* gene (mCherry: :moeABD) 17. MIG-2, F-actin, CED-10, and UNC-34 were all tightly localized to the basal invasive membrane of the AC both before and during AC invasion (Fig. 4a,d; Fig. S4; data not shown). This polarization was unique to the AC, as CED-10: :GFP and pan-uterine mCherry: :moeABD expression revealed that F-actin and CED-10 were not basally enriched in neighboring uterine cells (Fig. S4; data not shown). Examination of MIG-2, F-actin and UNC-34 indicated that, like UNC-40, their polarized localization was dependent on *unc-6* (Fig. 4b, e, j, k; data not shown), but not on the 1° vulval cue (Fig. 4c, f, j, k; data not shown). In contrast, PAR-3: :GFP, which localizes to apical and lateral membranes in wild-type ACs, and AJM-1: :GFP, which marks nascent apical spot junctions, were normal in *unc-6* mutants (Fig. S5). Thus, *unc-6* has a specific role in orienting downstream effectors to a specialized invasive cell membrane, but not in establishing the overall polarity of the AC.

Recently, the phospholipid phosphatidylinositol 4,5-bisphosphate ($PI(4,5)P_2$) has been implicated in linking the cortical actin cytoskeleton and Rac proteins to the inner plasma membrane leaflet 18,19. Strikingly, $PI(4,5)P_2$ (visualized with the PH domain from

Phospholipase C-δ fused to mCherry 20) was concentrated specifically at the basal invasive cell membrane of the AC (Fig. 4g, l), but was not polarized to the basal region of neighboring uterine cells (Fig. S6). In the absence of the 1° vulval cue, $PI(4,5)P_2$ was polarized (Fig. 4i, l), however, in *unc-6* mutants $PI(4,5)P_2$ was found throughout the AC plasma membrane (Fig. 4h, l). AC-specific sequestration of $PI(4,5)P_2$ (*cdh-3*>mCherry: :$PLC\delta^{PH}$) 18 caused delays in invasion and enhanced the invasion defects of both *unc-34* and *mig-2* mutants (Table S2). We infer that *unc-6* also promotes invasion through regulation of $PI(4,5)P_2$ localization at the invasive cell membrane.

We next examined the interaction of the *fos-1a* pathway with *unc-6* signaling. AC behavior in *fos-1a* mutants is distinct from *unc-6* animals. In *fos-1a(ar105)* mutants the AC extends cellular processes that flatten at the basement membrane, revealing a specific inability to breach this barrier 8. MIG-2: :GFP, marking the invasive membrane, was localized normally in *fos-1a* mutants, consistent with the ability of the AC to extend cellular processes (Fig. S7). Conversely, transcriptional reporters for *fos-1a* and two of its downstream targets, *zmp-1*, a matrix metalloproteinase, and hemicentin (*him-4*), a conserved extracellular matrix protein, were expressed normally in *unc-6* mutants (Fig. 5a, b; data not shown). In addition, *fos-1* RNAi treatment of *unc-40* mutants resulted in an increased block in AC invasion (Table S2), indicating that *fos-1a* has functions in AC invasion that are independent of the netrin pathway.

Notably, however, the *fos-1a* and netrin pathways intersect at the invasive cell membrane. A putative *zmp-1* null mutant has no invasion defect, and does not localize strongly to the invasive cell membrane, making its connection to *fos-1a* activity and basement membrane breakdown unclear 8. In contrast, null mutations in hemicentin cause a delay in AC invasion, and a functional hemicentin: :GFP transgene is assembled specifically under the invasive cell membrane of the AC, where it aids in basement membrane removal during invasion (Fig. 5c) 8. In *unc-6* mutants, there was a 65% reduction in hemicentin deposited under the invasive cell membrane (Fig. 5c, d) and a three-fold increase in hemicentin accumulation along lateral and apical membranes of the AC compared with wild-type controls (Video S1, S2). Lack of hemicentin is not sufficient to account for the severe block in AC invasion observed in *fos-1a* mutants, and another key downstream mediator(s) of *fos-1a* remains to be identified 8. Nevertheless, the failure of hemicentin to be deposited normally indicates that the activities of the *unc-6* (netrin) and *fos-1a* pathways intersect at the invasive membrane, and that other targets of *fos-1a* might similarly require *unc-6* for proper localization.

Taken together, our data demonstrate that UNC-6 generated from the VNC acts through its receptor UNC-40 in the AC to orient a specialized invasive membrane domain containing F-actin, actin regulators and the phospholipid $PI(4,5)P_2$ towards the basement membrane. Site of action and genetic studies support a model where UNC-6 and the vulval cue act independently on the AC to promote invasion, a notion further strengthened by the distinct role for UNC-6 in polarizing the invasive membrane. The failure of the AC to extend robust invasive processes towards displaced vulval cells suggests that formation of the invasive membrane domain is required to respond to the vulval cue. UNC-6 is also necessary for normal hemicentin deposition, a key *fos-1a* target 8. Thus, UNC-6 function is required for

the integration of multiple pathways that converge at the invasive cell membrane to promote invasion (summarized in Fig. 5e).

Netrins are involved in a wide array of developmental events, including axon guidance, cell migration, and synaptogenesis 9,10,21. These cellular processes have recently been proposed to share an early polarization event mediated by netrin signaling 21. Our work supports this idea and further suggests that netrin may function generally to specify subcellular domains by localizing phosphoinositide species such as $PI(4,5)P_2$, F-actin, and at least two of its major downstream effectors, UNC-34 (Enabled) and Rac GTPases. Consistent with this model, polarized UNC-40 within the HSN neuron in *C. elegans* is known to recruit another downstream effector, MIG-10 (Lamellipodin), a protein requiring phosphoinositides modified at the 3' position for membrane targeting 14.

Netrins have not previously been implicated in regulating cell invasions *in vivo*. Recent work, however, has shown that Netrin-1 is strongly associated with metastatic breast cancer, and stimulates invasion through collagen type I gels in colon cancer cells *in vitro* 22,23. Furthermore, netrins are potent angiogenic factors in vertebrates 24–26, a process that depends upon capillary sprouts invading through basement membrane 27. Our observations demonstrating a direct role for *unc-6* promoting cell invasion through basement membrane *in vivo* suggests that netrin is a conserved regulator of this process, and highlights the therapeutic potential of targeting netrin signaling to modulate cell-invasive behavior.

METHODS

Worm handling and strains

Wild-type nematodes were strain N2. Strains were reared and viewed at 20°C or 25°C using standard techniques. In the text and figures we refer to linked DNA sequences that code for a single fusion protein using a (: :) annotation. For designating linkage to a promoter we use a (>) symbol. The following alleles and transgenes were used: *qyEx78 [Venus: :unc-6(ΔSP)]*, *ghEx11[egl-17>rde-1: :mRFP]*, *ghEx13[egl-17>Venus: :unc-6]*, *ghEx18[glr-1>Venus: :unc-6]*, *qyEx60[fos-1a>mCherry: :PLCδ^{PH}]*, *qyIs25[cdh-3>mCherry: :PLCδ^{PH}]*, *qyIs61[cdh-3>GFP: :unc-34]*, *qyIs67[cdh-3>unc-40: :GFP]*, *syIs157[cdh-3>YFP)*, *zuIs20(par-3: :GFP);* **LGI**, *muIs27[GFP: :mig-2]*, *unc-40(e271)*; **LGII**, *qyIs17[zmp-1>mCherry]*, *qyIs23[cdh-3>mCherry: :PLCδ^{PH}]*, *rrf-3(pk1426)*, *syIs77(zmp-1>YFP);* **LGIII**, *ghIs8[Venus: :unc-6]*, *unc-119(ed4)*, *pha-1(e2123ts)*, *rhIs23[hemicentin: :GFP]*, *syIs129[hemicentin-ΔSP: :GFP];* **LGIV**, *ced-10(n1993)*, *jcIs1[ajm-1: :GFP]*, *lin-3(n1079)*, *lin-3(n378);* **LGV**, *fos-1(ar105)*, *rde-1(ne219)*, *unc-34(gm104)*, *qyIs50[cdh-3>mCherry: :moeABD];* **LGX**, *qyIs66[cdh-3>unc-40: :GFP]*, *qyIs7[lam-1: :GFP]*, *qyIs24[cdh-3>mCherry: :PLCδ^{PH}]*, *syIs59[egl-17>CFP]*, *kyIs299[hs>unc-6: :HA; unc-86>myr-GFP; odr-1>DsRed]*, *syIs50(cdh-3: :GFP)*, *mig-2(mu28)*, *unc-6(ev400)*. Vulvaless animals were created either through laser ablation or using the strain *lin-3(n1059)/lin-3(n378)* as described 5. The *hs>unc-6: :HA* transgenic worms (*kyIs299*) were grown at 15°C, conditions where it has been shown that UNC-6: :HA expression is not detectable 14. High levels of UNC-6: :HA were induced with a 2h heat

shock at 30°C as previously shown14. Table S1 may be consulted for a list of additional alleles examined.

Molecular biology and the generation of transgenic animals

Translational reporter constructs fusing coding sequences for GFP to the cDNAs encoding UNC-40 (*pUnc86>unc-40::GFP*), UNC-34 (*pUnc86> GFP::unc-34*), Laminin (pGK41), and CED-10 (pPR80) have been described 14,16,28. To label F-actin we created construct pJWZ6 by inserting a previously described *in vivo* actin binding probe from *Drosophila* Moesin 17 into a BamH1 site 3' to the coding sequences for mCherry (pAA64). A probe for PI(4,5)P2 (construct pAA173) was generated by cloning the PH domain from human Phospholipase C-δ 1 (Amino Acids 9–139) into a SpeI site 3' to the coding sequences for mCherry. To generate an *unc-6* reporter transgene (*Venus::unc-6(ΔSP))* that would indicate the cells in which UNC-6 message is transcribed, we modified a rescuing venus::unc-6 plasmid (*pVns-unc-6*)11 using a PCR fusion based strategy previously described 29. Primers were designed such that the nucleotides encoding the predicted signal peptide (AA 1–21) were removed during PCR fusion.

To prepare reporter constructs for AC- or uterine-specific expression, we employed PCR fusion to place each coding region into the context of a tissue specific promoter as previously described 8. For uterine specific expression we employed the *fos-1a* promoter 8 and for AC specific expression we utilized the AC specific *zmp-1*$^{mk50–51}$ or *cdh-3*$^{mk62–63}$ regulatory regions 8. We performed all fusions using either Phusion DNA Polymerase (New England Biolabs, Ipswich, MA) or the Expand Long Template PCR System (Roche Diagnostics, Indianapolis, IN). Templates and specific PCR primers for each promoter and reporter gene are listed in Table S4.

Transgenic worms were created by transformation with co-injection markers pPD#MM016B (*unc-119+*), pBX (*pha-1+*) or pPD132.102 (*myo-2>YFP*) into the germ-line of *unc-119(ed4), pha-1(e2123ts)*, or wild-type animals, respectively. These markers were injected with either EcoRI digested salmon sperm DNA, pBluescript II, or genomic *C. elegans* DNA at 40–100ng/μl to act as carrier DNA along with serial dilutions of the expression constructs to optimize expression levels and avoid toxicity. Transgenic extrachromosal (*Ex*) lines and integrated strains (*Is*) generated in this study are listed in Table S5. Integrated strains were generated as described previously 8.

Image acquisition, processing and analysis

Images were acquired using a Zeiss AxioImager A1 microscope with a 100X Plan-APOCHROMAT objective and a Zeiss AxioCam MRm CCD camera, controlled by Zeiss Axiovision software (Zeiss Microimaging Inc., Thornwood, NJ), or using a Yokogawa spinning disk confocal mounted on a Zeiss AxioImager A1 microscope using IVision software (Biovision Technologies, Exton, PA). Images were processed and overlaid using Photoshop 8.0 (Adobe Systems Inc, San Jose, CA), and 3-Dimensional projections were constructed using IMARIS 6.0 (Bitplane Inc., Saint Paul, MN).

Scoring of AC invasion, polarity, and fluorescence-intensity

AC invasion was scored as previously described 8. Polarity defects of *unc-6(ev400)* animals were determined by comparing average fluorescence intensity from five-pixel-wide linescans drawn along the invasive and non-invasive membranes of UNC-40: :GFP and mCherry: :moeABD in wild-type and mutant strains. To generate a polarity ratio, the fluorescence density of the invasive membrane was divided by the fluorescence density of the non-invasive membrane. This analysis showed a 3.3-fold enrichment of UNC-40: :GFP and a 4.0-fold enrichment of mCherry: :moeABD at the invasive membranes of wild-type animals. Loss of *unc-6* significantly perturbed AC polarity, reducing the polarity ratio by more than 50% for each marker ($P = 2\times10^{-7}$, unpaired *t*-test, $n = 20$ for each marker/genotype). Similarly, ectopic expression of UNC-6 significantly reduced polarity of UNC-40: :GFP by more than 40% when compared to controls ($P = 0.006$, $n = 15$ animals for each treatment). Other markers behaved consistently with these results. Through visual inspection of many wild-type and mutant animals, however, we determined that the diversity of polarity phenotypes of *unc-6* mutant animals was more accurately conveyed by grouping them into three phenotypic categories. These are reported in the figures and were grouped as follows: ACs containing a single intense region or fluorescence signal along the basal cortex/membrane were scored as “Polarized”; ACs with a roughly uniform distribution of fluorescence along all aspects of the cortex/membrane were scored as having “No Polarization”; ACs observed with a significant basal region of signal and with intense accumulations along apical or lateral faces were scored as “Apicolateral Accumulation”. In all cases the Fisher’s exact test was used to determine stastical significance for these analyses.

Mean fluorescence intensity of hemicentin deposition and AC expression of transgenic GFP reporter constructs in wild-type and *unc-6* mutants ($n = 18$ animals for each genotype) were calculated by sum projecting confocal z-series using Image J 1.40g software.

Laser ablation and P8.p isolation assay

Laser-directed cell ablations were performed on 5% agar pads as previously described 5. The attraction assay was carried out on strains NK212 (*syIs157[cdh-3>YFP]; syIs59[egl-17>CFP*]) and NK214 (*syIs157[cdh-3>YFP]; syIs59[egl-17>CFP*] *unc-6(ev400)*). AC invasion in both NK212 and NK214 without ablation yielded similar results to N2 and *unc-6(ev400)* mutants, respectively (n = 50 animals examined for each). Ablation of the VPCs P3.p through P7.p in both strains was performed at the early-to-mid L2 stage. Animals were then recovered from the agar pad used for ablation, allowed to develop at 20°C, and then examined for AC attraction to the P8.p cell and its descendants 18–24 hours after recovery.

Apical AJM-1 scoring in the AC

AJM-1: :GFP localization was observed in a single nascent spot junction in the apical region of the AC in wild-type animals beginning at the late P6.p 1-cell stage, approximately 3–4 hours prior to invasion. The number of spot junctions increased to approximately two by the P6.p 4-cell stage (range was from one to four). The number and apical position of spot

junctions was then compared in wild-type and *unc-6* mutants from the P6.p 1-cell stage through the P6.p 4-cell stage.

RNA interference

Double stranded RNA (dsRNA) against *fos-1* was delivered by feeding as previously described 8. To trigger vulval-cell specific knock-down of *unc-6* expression, *rde-1(ne219); ghEx11[egl-17>rde-1::mRFP]* worms were cultured on bacteria generating dsRNA targeting *unc-6* 11.

Supplementary Material

Refer to Web version on PubMed Central for supplementary material.

Acknowledgements

We are grateful to C. Bargmann for the *GFP::unc-34* and *unc-40::GFP* vectors, the *hs>unc-6::HA* integrated strain, and advice; W. Wadsworth for the Lam-1::GFP vector; E. Lundquist for the *GFP::ced-10* vector; Y. Goshima for Venus::unc-6 strains; D. Kiehart for the *moeADB::GFP* vector; the *Caenorhabditis* Genetics Center for providing strains; and N. Sherwood, Z. Wang, G. Lopez, G. Miley and D. Matus for comments on the manuscript. This work was supported by a Basil O'Connor Award, Pew Scholars Award, and NIH Grant GM079320 to D.R.S.

REFERENCES

1. Machesky L, Jurdic P, Hinz B. Grab, stick, pull and digest: the functional diversity of actin-associated matrix-adhesion structures. Workshop on Invadopodia, Podosomes and Focal Adhesions in Tissue Invasion. EMBO Rep. 2008; 9:139–143. [PubMed: 18202718]
2. Even-Ram S, Yamada KM. Cell migration in 3D matrix. Curr Opin Cell Biol. 2005; 17:524–532. [PubMed: 16112853]
3. Hotary K, Li XY, Allen E, Stevens SL, Weiss SJ. A cancer cell metalloprotease triad regulates the basement membrane transmigration program. Genes Dev. 2006; 20:2673–2686. [PubMed: 16983145]
4. Sharma-Kishore R, White JG, Southgate E, Podbilewicz B. Formation of the vulva in Caenorhabditis elegans: a paradigm for organogenesis. Development. 1999; 126:691–699. [PubMed: 9895317]
5. Sherwood DR, Sternberg PW. Anchor cell invasion into the vulval epithelium in C. elegans. Dev Cell. 2003; 5:21–31. [PubMed: 12852849]
6. Hwang BJ, Meruelo AD, Sternberg PW. C. elegans EVI1 proto-oncogene, EGL-43, is necessary for Notch-mediated cell fate specification and regulates cell invasion. Development. 2007; 134:669–679. [PubMed: 17215301]
7. Rimann I, Hajnal A. Regulation of anchor cell invasion and uterine cell fates by the egl-43 Evi-1 proto-oncogene in Caenorhabditis elegans. Dev Biol. 2007; 308:187–195. [PubMed: 17573066]
8. Sherwood DR, Butler JA, Kramer JM, Sternberg PW. FOS-1 promotes basement-membrane removal during anchor-cell invasion in C. elegans. Cell. 2005; 121:951–962. [PubMed: 15960981]
9. Baker KA, Moore SW, Jarjour AA, Kennedy TE. When a diffusible axon guidance cue stops diffusing: roles for netrins in adhesion and morphogenesis. Curr Opin Neurobiol. 2006; 16:529–534. [PubMed: 16935486]
10. Hedgecock EM, Culotti JG, Hall DH. The unc-5, unc-6, and unc-40 genes guide circumferential migrations of pioneer axons and mesodermal cells on the epidermis in C. elegans. Neuron. 1990; 4:61–85. [PubMed: 2310575]
11. Asakura T, Ogura K, Goshima Y. UNC-6 expression by the vulval precursor cells of Caenorhabditis elegans is required for the complex axon guidance of the HSN neurons. Dev Biol. 2007; 304:800–810. [PubMed: 17320069]

12. Wadsworth WG, Bhatt H, Hedgecock EM. Neuroglia and pioneer neurons express UNC-6 to provide global and local netrin cues for guiding migrations in C. elegans. Neuron. 1996; 16:35–46. [PubMed: 8562088]
13. Burdine RD, Branda CS, Stern MJ. EGL-17(FGF) expression coordinates the attraction of the migrating sex myoblasts with vulval induction in C. elegans. Development. 1998; 125:1083–1093. [PubMed: 9463355]
14. Adler CE, Fetter RD, Bargmann CI. UNC-6/Netrin induces neuronal asymmetry and defines the site of axon formation. Nat Neurosci. 2006; 9:511–518. [PubMed: 16520734]
15. Gitai Z, Yu TW, Lundquist EA, Tessier-Lavigne M, Bargmann CI. The netrin receptor UNC-40/DCC stimulates axon attraction and outgrowth through enabled and, in parallel, Rac and UNC-115/AbLIM. Neuron. 2003; 37:53–65. [PubMed: 12526772]
16. Lundquist EA, Reddien PW, Hartwieg E, Horvitz HR, Bargmann CI. Three C. elegans Rac proteins and several alternative Rac regulators control axon guidance, cell migration and apoptotic cell phagocytosis. Development. 2001; 128:4475–4488. [PubMed: 11714673]
17. Edwards KA, Demsky M, Montague RA, Weymouth N, Kiehart DP. GFP-moesin illuminates actin cytoskeleton dynamics in living tissue and demonstrates cell shape changes during morphogenesis in Drosophila. Dev Biol. 1997; 191:103–117. [PubMed: 9356175]
18. Janmey PA, Lindberg U. Cytoskeletal regulation: rich in lipids. Nat Rev Mol Cell Biol. 2004; 5:658–666. [PubMed: 15366709]
19. Heo WD, et al. PI(3,4,5)P3 and PI(4,5)P2 lipids target proteins with polybasic clusters to the plasma membrane. Science. 314:1458–1461.
20. Rescher U, Ruhe D, Ludwig C, Zobiack N, Gerke V. Annexin 2 is a phosphatidylinositol (4,5)-bisphosphate binding protein recruited to actin assembly sites at cellular membranes. J Cell Sci. 2004; 117:3473–3480. [PubMed: 15226372]
21. Colon-Ramos DA, Margeta MA, Shen K. Glia promote local synaptogenesis through UNC-6 (netrin) signaling in C. elegans. Science. 2007; 318:103–106. [PubMed: 17916735]
22. Fitamant J, et al. Netrin-1 expression confers a selective advantage for tumor cell survival in metastatic breast cancer. Proc Natl Acad Sci U S A. 2008; 105:4850–4855. [PubMed: 18353983]
23. Rodrigues S, De Wever O, Bruyneel E, Rooney RJ, Gespach C. Opposing roles of netrin-1 and the dependence receptor DCC in cancer cell invasion, tumor growth and metastasis. Oncogene. 2007; 26:5615–5625. [PubMed: 17334389]
24. Nguyen A, Cai H. Netrin-1 induces angiogenesis via a DCC-dependent ERK1/2-eNOS feed-forward mechanism. Proc Natl Acad Sci U S A. 2006; 103:6530–6535. [PubMed: 16611730]
25. Park KW, et al. The axonal attractant Netrin-1 is an angiogenic factor. Proc Natl Acad Sci U S A. 2004; 101:16210–16215. [PubMed: 15520390]
26. Wilson BD, et al. Netrins promote developmental and therapeutic angiogenesis. Science. 2006; 313:640–644. [PubMed: 16809490]
27. Heissig B, Hattori K, Friedrich M, Rafii S, Werb Z. Angiogenesis: vascular remodeling of the extracellular matrix involves metalloproteinases. Curr Opin Hematol. 2003; 10:136–141. [PubMed: 12579040]
28. Kao G, Huang CC, Hedgecock EM, Hall DH, Wadsworth WG. The role of the laminin beta subunit in laminin heterotrimer assembly and basement membrane function and development in C. elegans. Dev Biol. 2006; 290:211–219. [PubMed: 16376872]
29. Hobert O. PCR fusion-based approach to create reporter gene constructs for expression analysis in transgenic C. elegans. Biotechniques. 2002; 32:728–730. [PubMed: 11962590]

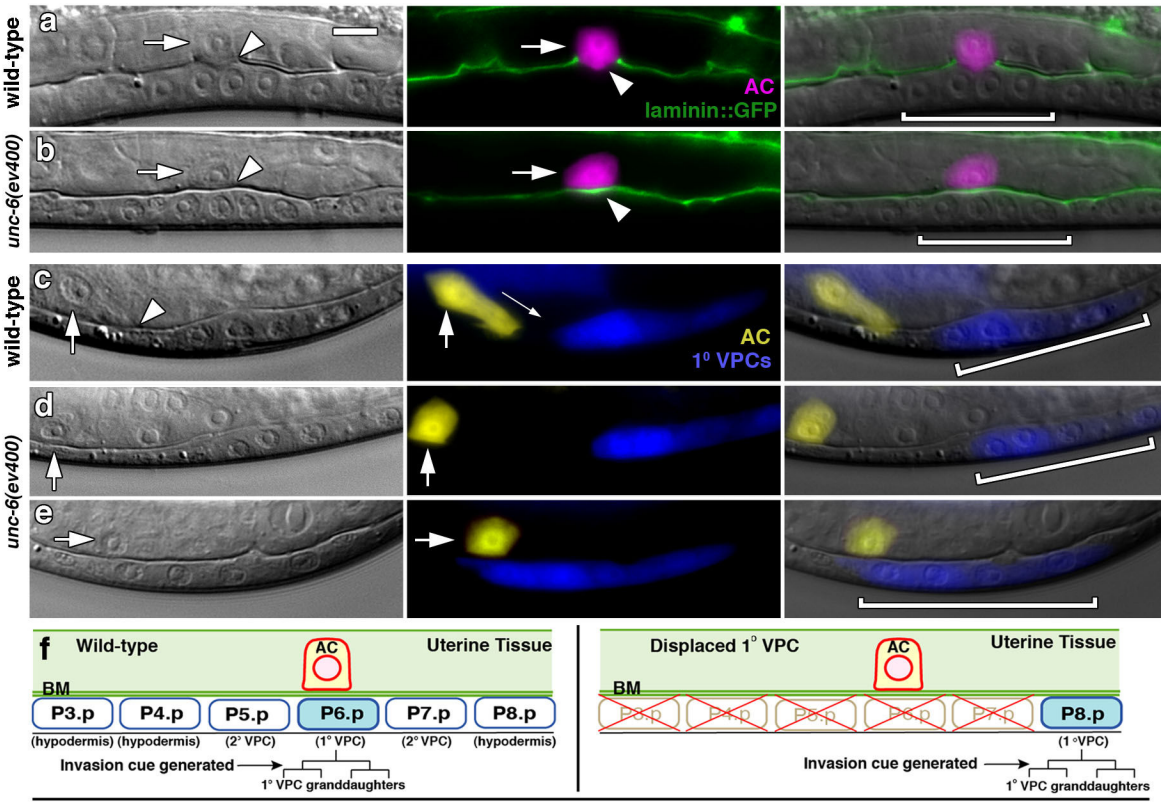

Figure 1. The AC fails to invade in *unc-6* (netrin) mutants

Late L3 animals; anterior left, ventral down; bracket, 1° VPCs. (**a**) Nomarski (left), fluorescence (center), and overlaid images (right) show that the wild-type AC (arrows; expressing *zmp-1*>mCherry in magenta) has crossed basement membrane (arrowhead; interruption of phase dense line on left and basement membrane component laminin, LAM-1: :GFP in green) and contacted the central 1° fated P6.p granddaughters (P6.p 4-cell stage; 20/20 animals). (**b**) In *unc-6* mutants, the basement membrane was intact under the AC in most animals (18/21 animals), and showed only small gaps in those that had partially invaded (3/21 animals, not shown). (**c**) In wild-type animals the AC (expressing *cdh-3*>YFP in yellow) extended invasive processes toward isolated 1° fated P8.p cell descendants (expressing *egl-17*>CFP in blue) in all cases examined (up to 25μm away; 42/42 animals). (**d**,**e**) In *unc-6* mutants the AC failed to extend invasive processes toward 1° fated P8.p cell descendants (44/44 animals), even when they directly bordered the AC (**e**, 9/9 animals). (**f**) Schematic diagram showing the AC in wild-type animals at the early L3 stage (P6.p 1-cell stage, left), and after ablation of the VPCs P3.p through P7.p (right). Both diagrams show animals prior to division of the 1° fated VPC (shown in blue). Future divisions of the 1° VPC prior to and during invasion are shown below in brackets. The arrow points to the time that the 1° VPC cue is generated that stimulates invasion. At this time the AC breaks through the underlying gonadal and ventral epidermal basement membranes (BM) and invades towards the 1° VPCs. The scale bar (upper left panel) is 5 μm for this and all other figures.

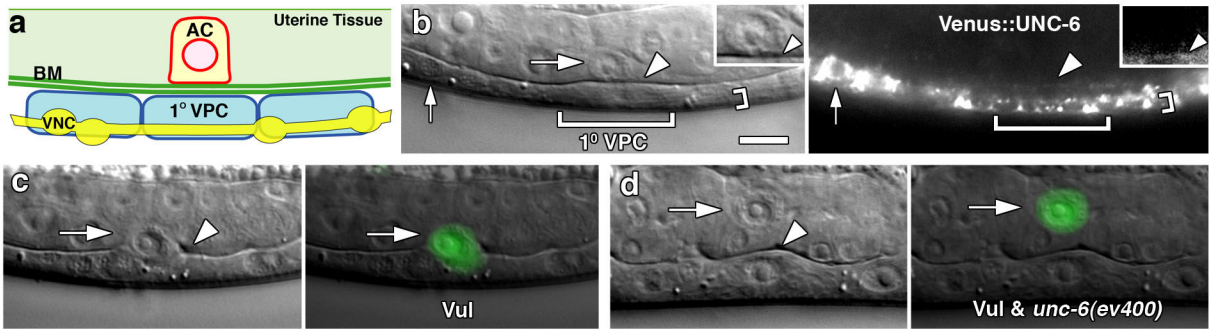

Figure 2. UNC-6 is a distinct VNC-derived pro-invasive cue

(**a**) A schematic image along the left side of the animal showing the relationship of the AC, basement membrane (BM), 1° VPC, and the neighboring ventral nerve cord (VNC) with associated cell bodies (yellow ovals). (**b**) Nomarski (left) and fluorescence (right) images of an animal expressing Venus::UNC-6 viewed at the focal plane between the 1° VPC (large bracket) and the VNC. Venus::UNC-6 accumulated in the VNC (small bracket, small arrow points to VNC cell body where accumulation was strongest), and low levels were found in the basement membrane underlying the AC (arrowheads). Insets show an enlarged image of the AC with Venus::UNC-6 localization ventrally in the basement membrane (arrowheads). (**c**) In approximately 20% of vulvaless animals the AC invades into the underlying epidermis (both in *lin-3* loss of function mutants or when removed by laser ablation; Table S2). A Nomarski image (left) and a *cdh-3*>GFP overlay (right) show an AC in a vulvaless animal (arrow) that has broken through the underlying basement membrane and invaded (arrowhead). (**d**) In vulvaless animals carrying the *unc-6* mutation, the AC never invaded (70/70 animals) and usually detached from the basement membrane at the early L4 stage (arrowhead; 65/70 animals; Table S2).

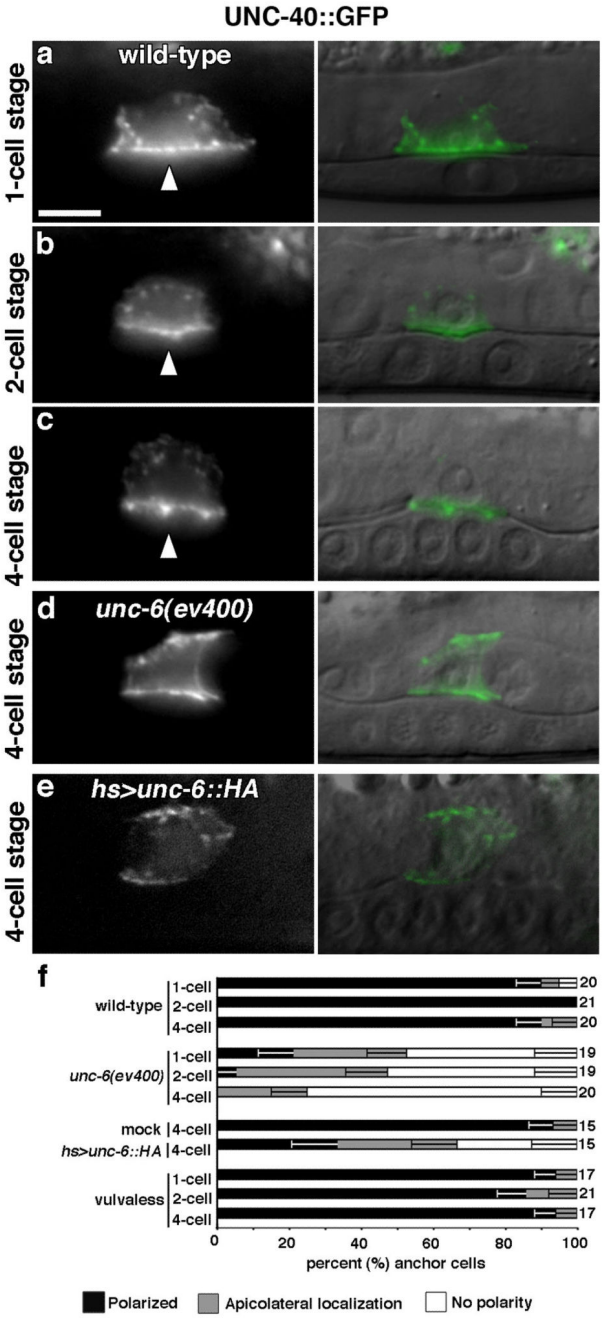

Figure 3. UNC-6 directs its receptor UNC-40 to the invasive cell membrane

Fluorescence image (left), Nomarski overlay (right). (**a-c**) UNC-40: :GFP was present within intracellular vesicles and polarized to the AC's invasive cell membrane (arrowheads) during the late L2 molt (P6.p 1-cell stage; 5–6 hours prior to invasion). UNC-40: :GFP maintained this polarization until the time of invasion at the P6.p 4-cell stage. (**d**) UNC-40: :GFP polarization was perturbed in *unc-6* mutants, and (**e**) in wild-type animals ubiquitously expressing UNC-6: :HA induced by heat shock. (**f**) Compared with wild-type controls, UNC-40: :GFP polarization in *unc-6* mutants, or following ubiquitous UNC-6: :HA

expression was significantly perturbed ($P < 7\times10^{-4}$ in all cases, Fisher's exact test in this and subsequent graphs). In contrast, neither vulvaless nor mock heat shocked animals showed changes in UNC-40: :GFP polarity compared with wild-type ($P > 0.05$). The number of animals examined at each stage is listed to the right of the graph; error bars report the standard error of the proportion.

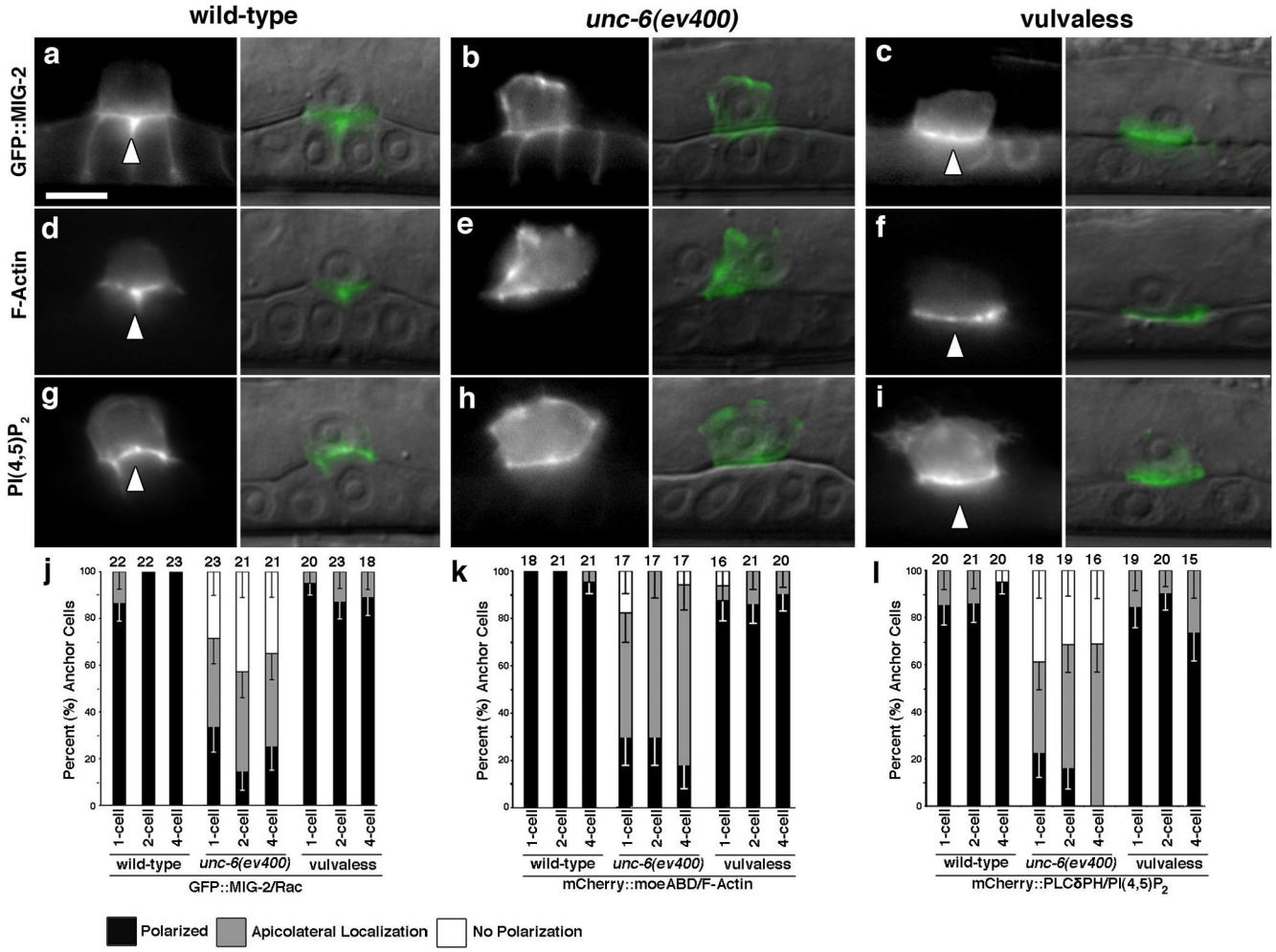

Figure 4. UNC-6 localizes the Rac protein MIG-2, F-actin, and PI(4,5)P_2 to the invasive cell membrane

Fluorescence image (left), Nomarski overlaid image (right). (**a**, **d**, **g**) The Rac protein GFP: :MIG-2, the F-actin binding protein mCherry: :moeABD and the phosphatidylinositol 4,5-bisphosphate sensor mCherry: :PLCδ^{PH} were localized to the invasive cell membrane in wild-type animals (arrowheads). The endogenous *mig-2* promoter also drove low levels of expression in the vulval cells. (**b**, **e**, **h**) In *unc-6* mutants, MIG-2, F-actin and PI(4,5)P_2 failed to polarize to the invasive cell membrane. (**c**, **f**, **i**) In contrast, MIG-2, F-actin and PI(4,5)P_2 were polarized normally in vulvaless animals (arrowheads). (**j**, **k**, **l**) Quantification of MIG-2, F-actin and PI(4,5)P_2 polarization, respectively, in wild-type, *unc-6*, and vulvaless animals prior to and during invasion. Localization of all markers was significantly perturbed in *unc-6* animals at all time points examined compared to wild-type controls (P >0.0003 in all cases). In contrast, vulvaless animals showed no significant changes in polarity (P > 0.05). The number of animals examined at each stage is noted at the top of each bar; error bars show the standard error of the proportion and raw percentages are reported in Table S3.

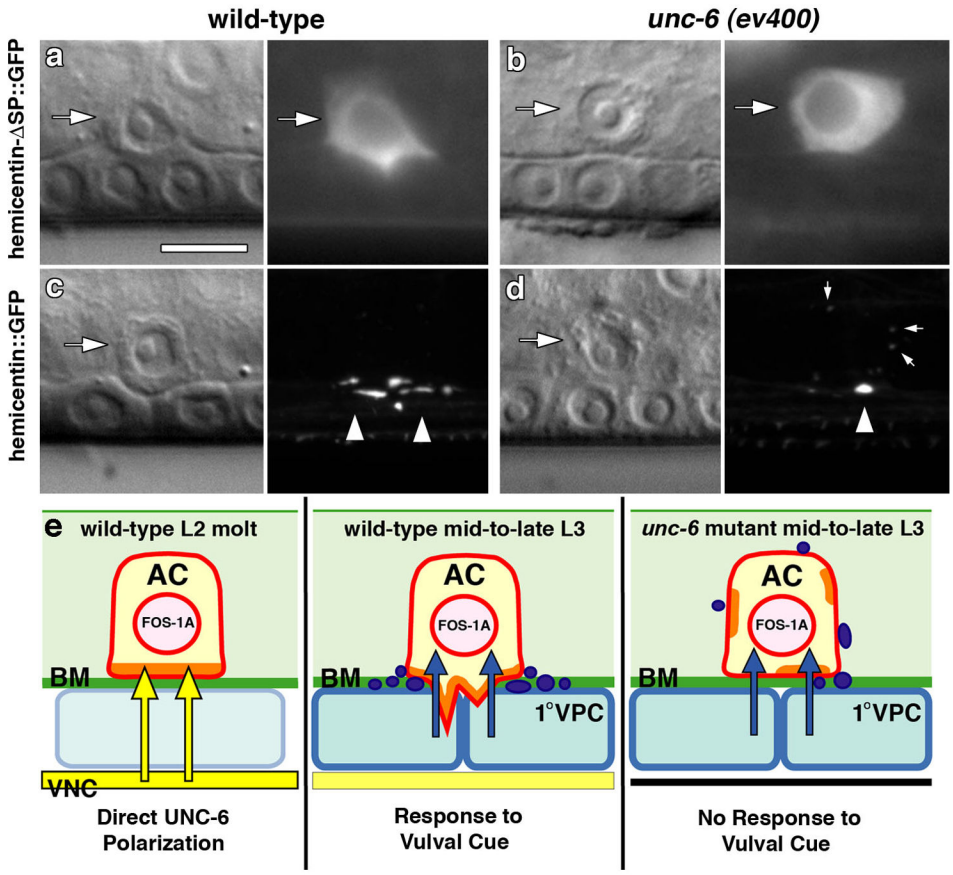

Figure 5. UNC-6 promotes the deposition of hemicentin at the site of invasion

Nomarski images (left) and corresponding fluorescence images (right). (**a**) Expression of the transcriptional reporter hemicentin-ΔSP: :GFP within the AC (arrow) in wild-type animals during invasion. (**b**) Hemicentin-ΔSP: :GFP was expressed at the same levels in *unc-6* mutants (n = 20 for each; P = 0.69, unpaired t-test). (**c**) Full length hemicentin: :GFP is deposited under the AC's invasive membrane (arrowheads) during invasion. (**d**) In *unc-6* mutants, there was a 65% reduction in hemicentin deposition under the invasive cell membrane (arrowhead; $P = 5.0\times10^{-6}$, unpaired t-test), and a three fold increase in accumulations formed along apical and lateral membranes (small arrows; P = 0.022, unpaired t-test, n = 18 for each; Videos S1, S2). We found no significant correlation (correlation coefficient = −0.248, P = 0.320 Students t-test, df = 16) between perturbations in hemicentin deposition and the contact area with the basement membrane. (**e**) Schematic diagram of the role of *unc-6* (netrin) in regulating AC invasion. During the L2 molt, UNC-6 protein secreted from the ventral nerve cord (VNC and arrows in yellow) polarizes its receptor UNC-40 to the AC's plasma membrane in contact with the basement membrane (BM, green). There, UNC-40 establishes a specialized invasive membrane domain (orange) containing F-actin, and its effectors--actin regulators and the phospholipid $PI(4,5)P_2$. Approximately 4–6 hours later, hemicentin is deposited under the invasive cell membrane (puncta, purple) and invasive protrusions are generated in response to the 1° vulval cell cue (VPCs, arrows in blue). In *unc-6* mutants, the invasive membrane is not polarized,

hemicentin deposition is reduced and mistargeted, and the AC fails to generate invasive processes in response to the 1° VPC signal. Importantly, this model for UNC-40 localization does not preclude the possibility of feed-back mechanisms that regulate UNC-40 localization and function.